Effect of Wave Interactions on Pressure Distributions in Supersonic and Hypersonic Flow

G. A. Bird*
University of Sydney, Sydney, Australia

The pressure distribution over a body of complex shape may be affected by the reflected waves that arise when the wave from a discontinuity in surface slope interacts with the bow shock or expansion wave, the entropy gradient behind a curved bow shock, or the effective area change with distance from the axis in axisymmetric flow. The reflected waves from all these types of interaction are examined by reflection coefficients based on the overall strength of the reflected waves or on the overall change in surface pressure, and also by calculations of the full inviscid flow field by the method of characteristics.

Nomenclature

d = distance along surface
p = pressure
p_i = pressure on surface immediately downstream of discontinuity in slope
p_∞ = pressure indefinitely far downsteam on a surface of constant slope
r_b = radius of blunt nose (cylindrical or spherical)
r_c = radius of cylindrical body
r_s = nose radius of detached shock wave
x = distance parallel to the freestream
y = distance normal to the freestream
M = flow Mach number
δ = surface deflection angle
$\epsilon, \epsilon', \epsilon''$ = reflection coefficients
θ = flow inclination angle
θ_w = shock wave angle
γ = specific heat ratio
μ = Mach angle
τ = thickness parameter

Subscript

f = denotes the freestream

Introduction

MANY methods[1] for calculating the inviscid pressure distribution over bodies in supersonic or hypersonic flow require only a knowledge of the local surface slope and the freestream conditions. These include the linearized method for two-dimensional supersonic flow, the tangent wedge and cone methods, and the various Newtonian impact methods. The shock-expansion method is a slight exception in that, as well as the local surface slope at any point, it requires the flow conditions at the immediately preceding point. The linearized method gives good results for thin pointed two-dimensional bodies at low incidence in supersonic flow, and the shock-expansion method gives excellent results for similar bodies in supersonic flow and reasonable results into the hypersonic regime for smooth bodies.[2] The other methods apply only to hypersonic flows and give reasonably good results for smooth shapes.

However, as shown in Fig. 1, any discontinuous change in slope on a body produces a finite wave (shock or expansion) that interacts with the upstream portion of the flow field. Reflected waves are produced in this interaction, and these may affect the surface pressure distribution downstream of the discontinuity in slope. None of the foregoing methods is able to provide an estimate of this effect.

The simplest type of interaction is the intersection of the two shock waves produced by a double wedge body as shown in Fig. 1a. A reflected wave and a contact surface form at the point of intersection, and a reflection coefficient may be defined as the ratio of the pressure difference across the reflected wave to that across the incident wave. An analytical expression has been found[3, 4] for this reflection coefficient for the limiting case of very weak waves, and the results have been used to investigate[1, 2] the probable accuracy of the shock-expansion method. When this second (or incident) shock is of finite strength, the reflection coefficient must be calculated numerically, and comprehensive results of such calculations are presented in this paper.

The reflection of an expansion wave from a shock wave (or vice versa) is less straightforward, since an expansion wave has a finite width and the intersection occupies a finite region. However, if both the waves are regarded as discontinuities, a solution may be obtained in the same manner as for the two shock intersections, and this gives the overall strength of the waves. This solution must be regarded as asymptotic, since the interaction extends downstream indefinitely as a result of the interaction of the reflected waves with the entropy gradient produced by the curved shock. The form of the reflection coefficient for these interactions also is discussed.

When considering the effect of these reflected waves on the surface pressure distribution, account must be taken of the multiple reflection of the waves between the surface and the shock wave. It then becomes convenient to base the reflection coefficient not on the overall strength of the reflected wave but on the overall pressure change on a flat surface following the discontinuity that produces the incident wave. This is calculated easily since the surface pressure must dent asymptotically to the value that would be appropriate to a surface of this slope if the initial part of the body, between the leading edge and the discontinuity, did not exist. For practical purposes, it is important to determine, in addition to this modified reflection coefficient, the rate at which the asymptotic surface pressure is approached. Therefore, as well as the results for the reflection coefficient, some results are given of calculations by the method of characteristics of the complete flow field.

In the case of a body with a blunt nose, strong reflected waves may be produced when the incident wave from a discontinuity crosses the entropy gradient from the curved bow shock. This type of interaction is shown in Fig. 1c, and the reflected waves may be important even when the incident shock does not intersect the bow shock in the region of interest. The asymptotic strength of these waves is investigated by reflection coefficients, and the method of character-

Received by IAS May 28, 1962; revision received October 16, 1962. This research was supported by the U. S. Air Force under Grant AF-AFOSR-61-93, monitored by the Air Force Office of Scientific Research of the Office of Aerospace Research.

* Senior Lecturer, Department of Aeronautical Engineering.

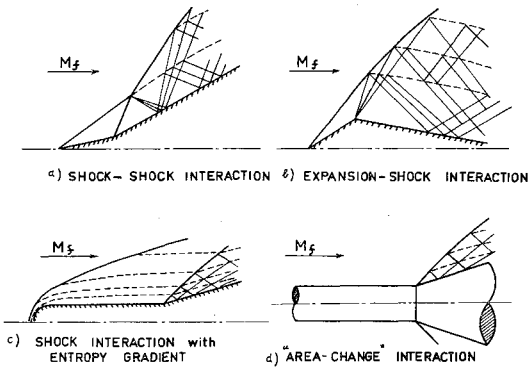

Fig. 1 Types of wave interaction

istics again is used to determine the rate at which these conditions are approached.

Although considerations have been confined to two-dimensional flow so far, the effects of axial symmetry also may be regarded as being due to a type of wave interaction. For instance, in the flow over the cylinder-flare shown in Fig. 1d, the pressure at the beginning of the flare would correspond to the two-dimensional value appropriate to the angle of the flare and then would tend asymptotically to the appropriate conical value. This pressure change may be regarded as being due to reflected waves that are generated as the shock interacts with the increase in flow area with distance from the axis. This type of wave interaction is investigated by calculations of the pressure distribution along conical flares and boattails.

The calculations have been made for the inviscid flow of a perfect gas. The full extent to which viscous effects would affect the actual flows could be determined only by experiment. It is unlikely that some of the flows for which inviscid solutions are presented could be realized in practice without some form of boundary layer control. Results are presented for a number of values of the specific heat ratio, so that it is possible to make at least a qualitative estimate of real gas effects.

Although detailed pressure distributions have been calculated only for two-dimensional and axisymmetric flows, the relative magnitudes of the various reflection coefficients should be of some help when estimating the pressure distributions over complex three-dimensional bodies in hypersonic flow. The overall results are discussed in the final section of the paper, and general conclusions are made about the effects of wave interactions on pressure distributions.

Shock and Expansion Wave Interactions

If an oblique shock wave is produced by a deflection of a stream through the angle δ_1 and a second shock of the same

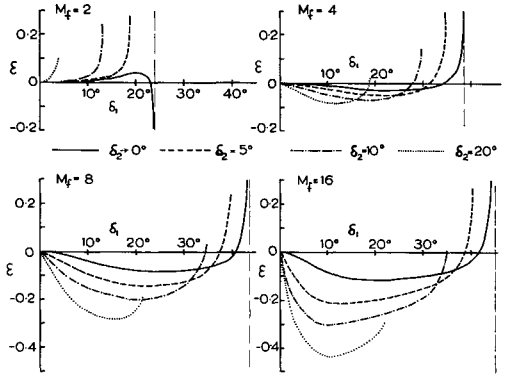

Fig. 2 Effect of Mach number on the two-shock reflection coefficient ($\gamma = \frac{7}{5}$)

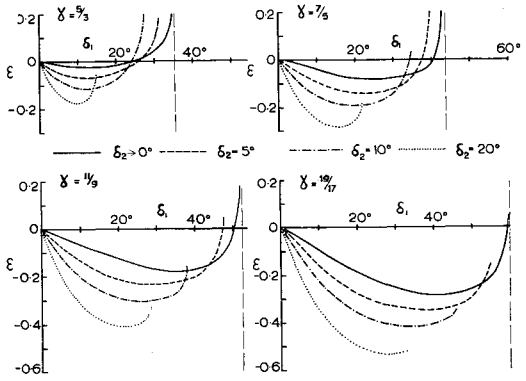

Fig. 3 Effect of specific-heat ratio on the two-shock reflection coefficient ($M_f = 8$)

family is produced by a further deflection δ_2, the two shocks must intersect, giving rise to a reflected wave of the opposite family. Courant and Friedrichs[5] present a graphical or numerical method for obtaining the strength of this reflected wave from the configuration of the wave polars in the pressure-flow velocity (or p-θ) plane. The strength of this reflected wave is conveniently related to that of the second (or incident) shock by the reflection coefficient ϵ, which was introduced by Chu[4] and is defined as the ratio of the pressure difference across the reflected wave to that across the incident wave.

Figure 2 shows† curves of ϵ for fixed values of δ_2 as a function of δ_1 for a number of values of freestream Mach number and $\gamma = \frac{7}{5}$. Figure 3 shows similar curves for a fixed Mach number and variable specific heat ratio. The reflection coefficient increases with Mach number and is highly sensitive to γ, becoming very large as γ tends to unity.

The solid lines correspond to the case when $\delta_2 \to 0$, and the incident wave becomes vanishingly weak. This solution depends only on the relative slopes of the wave polars at their point of intersection and, as stated earlier, has been obtained analytically.[3, 4] The reflection coefficient for very weak waves generally is small and negative, except when δ_1 approaches the shock detachment angle corresponding to M_f when it becomes large and positive. For finite values of δ_2, the reflection coefficient may increase with δ_2 very markedly in the regions where it is negative, and the positive regions tend to disappear. The curves for $M_f = 8$ and $\gamma = \frac{7}{5}$ are shown in greater detail in Fig. 4, and it is seen that, for a given δ_2, there is a limiting value of δ_1 beyond which a solution cannot be obtained by the wave polar method. This is

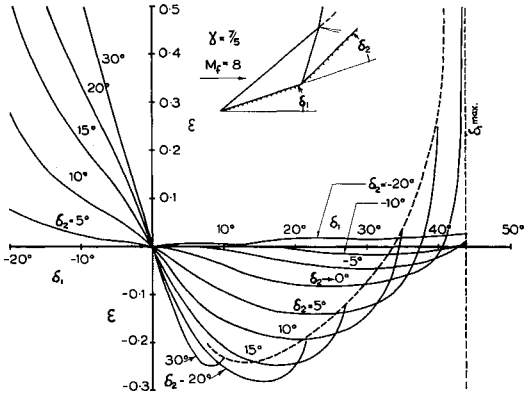

Fig. 4 Reflection coefficients for general two-wave interactions

† All the numerical computations for this paper were carried out using the SILLIAC digital computer at the University of Sydney.

Table 1 Region of unaffected pressure downstream of discontinuity

M_f \ δ_1	d/d_1 for $\delta_2 \to 0$, $\gamma = \frac{7}{5}$					
	5°	10°	15°	20°	30°	40°
2	11.72	5.41	3.14	1.64		
4	8.47	4.23	2.86	2.19	1.47	
8	4.57	2.44	1.82	1.54	1.26	0.94
16	2.48	1.60	1.37	1.28	1.16	0.95
	d/d_1 for $M_f = 8$, $\delta_1 = 15°$, $\gamma = \frac{7}{5}$					
δ_2	0°	5°	10°	20°	30°	40°
d/d_1	1.82	1.02	0.65	0.35	0.23	0.14

because the reflected wave polar no longer intersects the polar of the first (or bow) shock wave.

It is interesting to note that, at hypersonic speeds, the incident shock polar extends to much larger angles and pressures than the bow shock polar. Therefore, there may be an attached shock on a surface of slope such that a detached shock would result if it were exposed directly to the stream. The pressure on such a surface could be several times the magnitude of the blunt body stagnation pressure that would occur behind a normal shock wave in such a flow. Experiments in a supersonic wind tunnel at the University of Sydney have verified that the shock may remain attached to the leading edge of the second surface even though the slope of this surface is above the shock detachment angle of the bow shock polar.

As stated in the Introduction, interactions involving an expansion wave and a shock wave are not as straightforward as those between two shocks, since the interaction covers a large region in the physical plane. However, in the p-θ plane, solutions may be obtained from the wave polars just as readily as for the two shock case. These solutions effectively regarded all the waves as discontinuities and must give correctly the overall strengths of the waves. The typical form of the reflection coefficient curves for these interactions is shown in Fig. 4.

The reflection of an expansion wave from a shock results in weak reflected waves that may form either a net expansion or compression. However, when δ_1 is negative and δ_2 is positive, which corresponds to a shock being reflected from an expansion, the pressure change across the reflected wave even may exceed that across the shock wave. These large reflection coefficients result when the shock occurs in a region of very low pressure so that, although there is a large pressure ratio across the shock, the change in pressure is small compared with the total pressure change across the reflected waves.

Effect on Pressure Distribution

In any of the shock and expansion wave interactions there is a region of length d downstream of the discontinuity which is not affected by the reflected waves. The ratio of this length to the length d_1 of the initial portion of the surface of slope δ_1 is determined easily for the two shock case as

$$\frac{d}{d_1} = \left\{\frac{\cot(\theta_{w_2} - \delta_2) + \cot\mu_3}{\cot(\theta_{w_1} - \delta_1) - \cot\theta_{w_2}}\right\} \frac{\sin(\theta_{w_2} - \delta_2)}{\sin\theta_{w_2}}$$

θ_{w_1} and θ_{w_2} are the wave angles of the bow and incident shocks, respectively, and μ_2 and μ_3 are the Mach angles of the flow behind the bow and incident shocks. Some typical results for d/d_1 are shown in Table 1. First, the effect of freestream Mach number M_f and the initial deflection δ_1 is determined for very weak incident waves. Increases in M_f and δ_1 both cause the unaffected region to diminish. Also an increase in the strength of the incident wave, for constant M_f and δ_1, is shown to produce a marked reduction in the length of this region.

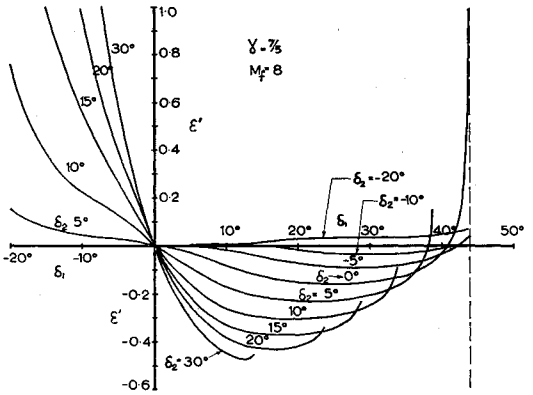

Fig. 5 Modified reflection coefficient based on overall change of surface pressure

Even when the reflected wave or waves impinge on the surface, the reflection coefficient ϵ that was used in the previous section does not give the complete story because the reflected waves are further reflected backward and forward between the surface and the shock. Additional rereflected waves result from the interaction of these waves with the entropy discontinuities and gradients that are set up as soon as the shock wave strengths vary. However, if the surface slope behind the discontinuity that produces the second or incident wave remains constant, the pressure along this surface must tend asymptotically to the pressure p_∞ that would occur on a surface of this slope exposed directly to the freestream. A modified reflection coefficient ϵ' may be defined as the ratio of the difference between p_∞ and the pressure p_i immediately downstream of the discontinuity to the pressure difference across the incident shock. Figure 5 gives the curves of ϵ' which correspond to those for ϵ in Fig. 4. The two sets of curves have a similar form, and the magnitude of ϵ' is everywhere of the order of twice that of ϵ. This is as would be expected from the relative locations of the points in the p-θ plane, and the general conclusions about the behavior of ϵ which were made from Figs. 2 and 3 apply also to ϵ'.

From the practical point of view, it is important to know the form of the pressure variation between the pressure p_i immediately behind the second wave and the asymptotic pressure p_∞, and also the rate at which p_∞ is approached. Therefore, the method of characteristics[1] was used to compute the complete flow field in some typical cases. All of these cases were for $\delta_1 = 15°$ and $\delta_2 = 30°$ (i.e., the reflection of a shock wave from an expansion), and the results are shown in Fig. 6. This configuration was chosen partly for ease of computation and partly because of the high values of ϵ'. Although this particular interaction would be affected in practice by viscous effects, these inviscid results should be similar to those for the other interactions.

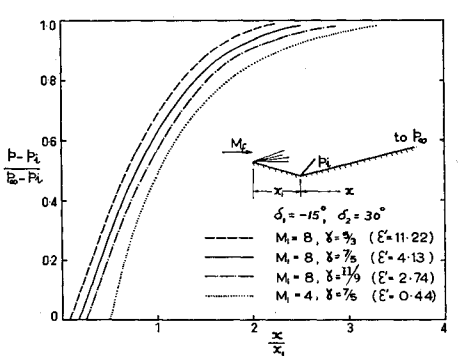

Fig. 6 Surface pressure distribution downstream of discontinuous change in slope

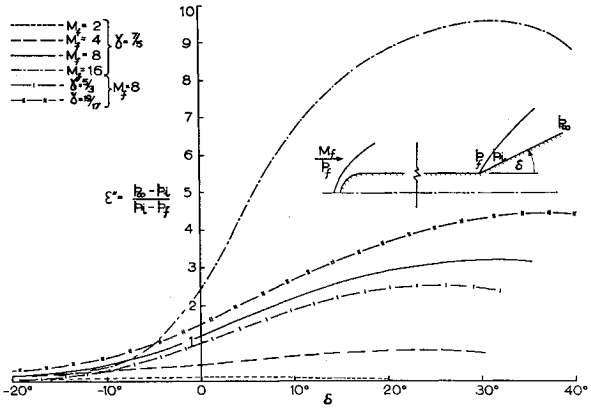

Fig. 7 Reflection coefficients for wave interaction with blunt-nose entropy gradient

It is seen that the asymptotic pressure is reached effectively in a distance equal to several times the length of the initial part of the surface. This distance is mainly a result of the finite width of the expansion, and, for the interaction of two shocks, the asymptotic pressure probably would be reached even more quickly.

Entropy Gradients from Blunt Nose

When a discontinuous change in slope occurs on a two-dimensional body that has a blunt leading edge, the resulting wave interacts with the entropy gradient from the curved bow shock wave. Reflected waves are produced, and the pressure distribution downstream of the change in slope is affected.

A convenient way of assessing the magnitude of this effect is to assume that the leading edge is cylindrical followed by a parallel section and that the change in slope is situated well back from the leading edge where the pressure has returned effectively to the freestream value p_f. The surface streamline passes through the normal shock at the apex of the bow shock, is compressed isentropically to the stagnation point, and then expands isentropically back to p_f. It follows from the normal shock and the isentropic flow equations[5] that the Mach number at the surface is

$$M = \left[\frac{\gamma+1}{\gamma-1} M_f^2 \left(\frac{2\gamma}{\gamma+1} M_f^2 - \frac{\gamma-1}{\gamma+1}\right)^{-1/\gamma} - \frac{2}{\gamma-1}\right]^{-1/2}$$

The initial pressure on the surface of slope δ then may be calculated from the oblique shock or Prandtl-Meyer expansion relationships. If this surface of slope δ is indefinitely long, the pressure along it must eventually tend to that which would occur on a surface of this slope exposed directly to a freestream of Mach number M_f. This pressure again will be denoted by p_∞, and a reflection coefficient for the interaction of a wave with an entropy gradient may be defined by

$$\epsilon'' = (p_\infty - p_i)/(p_i - p_f)$$

This is effectively the ratio of the total change in pressure across the reflected waves to the change in pressure at the discontinuity in slope.

Values of ϵ'' are plotted as a function of the deflection angle δ in Fig. 7. At low supersonic Mach numbers, ϵ'' is small compared with unity and is relatively unaffected by the sign or magnitude of δ. In the hypersonic region, ϵ'' remains small for strong expansion waves but increases rapidly with δ until near the shock detachment point.

It is again desirable to know the rate at which the asymptotic pressure is reached, and, to do this, it is necessary to know the Mach number variation with distance from the surface. This depends on the shape of the bow shock wave, and, for the purpose of these calculations, this has been assumed to be a hyperbola with a slope tending asymptotically to the freestream Mach angle. The slope of such a hyperbola at distance y from the axis is given by

$$dy/dx = [(r_s/y)^2 + (M_f^2 - 1)^{-1}]^{1/2}$$

The appropriate nose radius of the hyperbola r_s for a given nose radius of the body may be found from existing numerical solutions.[6] This shock then is divided into a number of small (streamtube) elements, and the oblique shock relations are used to find the pressure, Mach number, and area of each streamtube immediately behind the wave. Finally, the isentropic relations give the area and Mach number of each streamtube when the pressure has returned to the freestream value. The Mach number distribution normal to a point well downstream on the body surface then is known, and some results are shown in Fig. 8.

This enables the method of characteristics to be used to calculate the pressure distribution along the inclined surface downstream of the discontinuity. Some typical results are shown in Fig. 9. The distance x is measured in the direction of the freestream and is made nondimensional by dividing it by the nose radius of the body. At the low supersonic Mach numbers, for which ϵ'' is very small, the asymptotic pressure is attained effectively at an x/r_b of about 20. However, at hypersonic speeds, the initial pressure hardly is changed over distances of this order. There are two primary reasons for this effect. The first is that, as shown in Fig. 8, the freestream Mach number is approached much more slowly at hypersonic speeds that at supersonic speeds. Secondly, the Mach angles are very small at hypersonic speeds so that, at a given x/r_b, the surface pressure is influ-

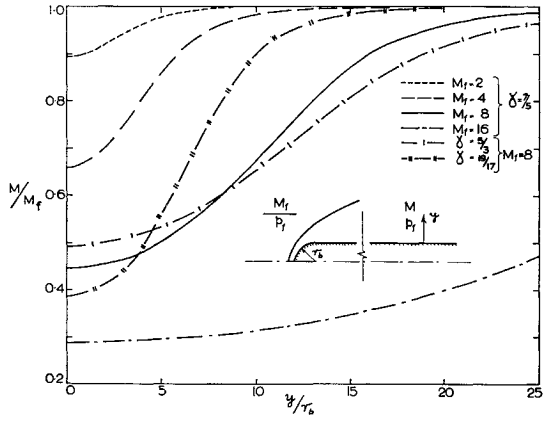

Fig. 8 Mach number distribution normal to the surface well downstream on blunt body

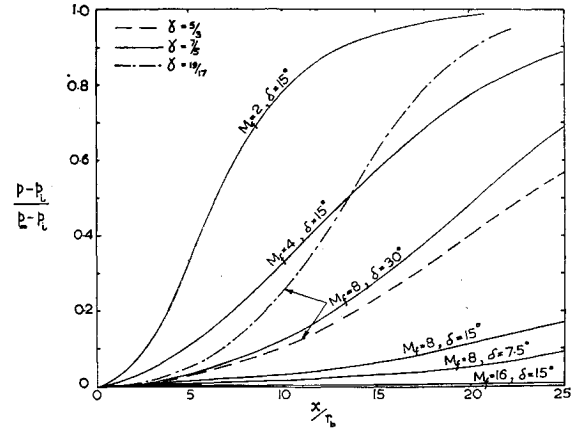

Fig. 9 Surface pressure downstream of discontinuity blunt-nosed body

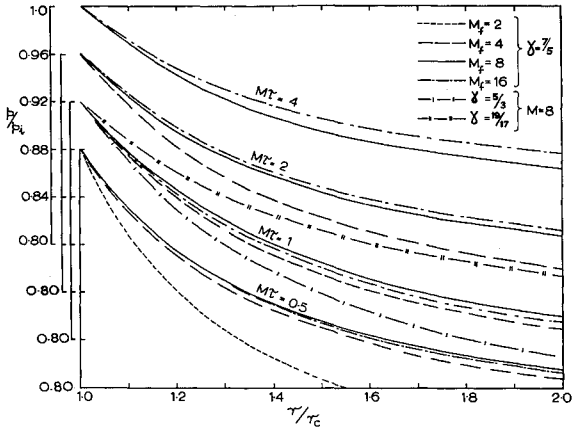

Fig. 10 Pressure distributions along conical flares following a long, sharp-nosed cylinder

enced by less of the external flow than would be the case at lower speeds. The results in Fig. 9 are all for a deflection of $+15°$, and this influence of the low Mach angle would be even more marked for negative deflection angles.

Axisymmetric Flows

As stated in the Introduction, the effects of axial symmetry may be regarded as being due to the interaction of waves with area change. Consider first the flow over a cylinder-conical flare combination. If the nose of the cylinder is very sharp (so that the entropy rise across the bow shock is negligible) and the flare is set sufficiently far back along the cylinder, the flow in front of the shock wave from the flare will have returned effectively to the freestream conditions. The initial pressure p_i on the flare is then the two-dimensional value appropriate to the cone semi-angle, and the pressure subsequently tends asymptotically to the conical value. The method of characteristics has been used to calculate the pressure distribution along such flares, and the results are shown in Fig. 10. The pressure has been plotted as a function of the radial distance from the axis for a number of values of the hypersonic similarity parameter M tanδ (or $M\tau$). For a given $M\tau$ and γ, the various curves collapse quite well for sufficiently high Mach numbers, and, in fact, many of the curves for different values of $M\tau$ are so similar that the origin has been shifted for each set of curves.

Similar calculations have been carried out for cylinder boattail combinations, and the results are plotted in Fig. 11. The positive pressure gradient along the boattail becomes very large when the radius is reduced to about one quarter of the radius of the cylinder, but, in practice, viscous

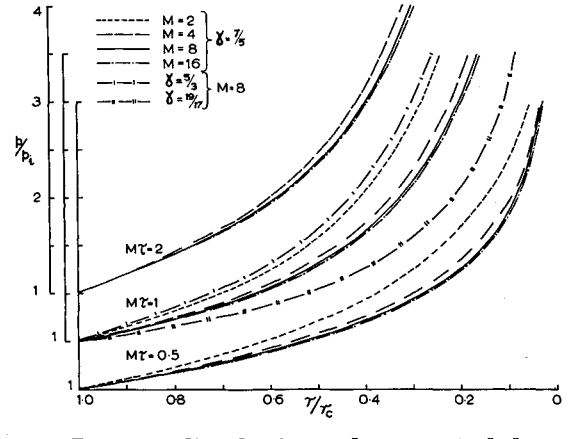

Fig. 11 Pressure distributions along conical boattails following a long, sharp-nosed cylinder

effects usually will cause separation well upstream of this radius.

If the cylinder has a blunt nose, effects similar to those investigated in the previous section for two-dimensional flows will be encountered. Also, if the cylinder were too short for the surface pressure to have returned effectively to the freestream value, the surface pressure for the blunt nosed bodies would be higher than the freestream pressure (see, e.g., Ref. 7), and the flow Mach number at the surface would be correspondingly less. In addition, the shock wave from the flare or the expansion wave from the boattail might interact with the bow shock wave and produce reflected waves of the type discussed earlier.

Discussion and Conclusions

When two shock waves of the same family intersect in two-dimensional flow, the reflected wave is normally an expansion. The reflection coefficients increase with the strength of the second (or incident) wave and may become three or four times larger than the previously determined[3, 4] reflection coefficients for very weak incident waves. The reflection coefficients increase with the freestream Mach number. This increase is particularly marked in the transition from supersonic to hypersonic flow, and the reflected waves do not have a significant effect at the lower supersonic Mach numbers. The reflection coefficients also increase as the specific heat ratio is reduced. This indicates that high temperature real gas effects will accentuate the importance of these reflected waves in hypersonic flows.

The reflection coefficients for the reflection of an expansion wave of finite strength from a shock wave are much smaller in magnitude than those for the reflection of a very weak expansion wave. In some cases, the reflection coefficient is opposite in sign to that for the corresponding very weak wave. This provides a very simple means of verifying the conclusion[1, 2] that the shock-expansion method is accurate at hypersonic speeds for smooth two-dimensional aerofoils (which always involve the reflection of an expansion from a shock). This conclusion does not necessarily hold for more complex shapes, since the reflection coefficient for the reflection of a finite strength compression from a shock is much larger than that for a very weak wave, and the reflection coefficient for a shock wave from an expansion wave easily may exceed unity.

The reflection coefficients give the magnitude of the pressure change due to the reflected waves on a surface that extends infinitely far downstream. At low supersonic Mach numbers, the reflected waves produced by the wave from a surface discontinuity may not reach the surface for a considerable distance downstream of the discontinuity, and, depending on the geometry, they may miss the surface altogether. However, when the discontinuity produces a shock wave, this distance decreases sharply with increasing Mach number and with the strength of the incident wave. The reflected waves from an incident shock will, therefore, often intersect the surface in a hypersonic flow field. The reflected waves from an incident expansion wave are less likely to reach the surface in practical configurations, but, for this interaction, the reflection coefficients are very small. In general, the probability of the reflected waves affecting the surface pressure distribution increases with the magnitude of the reflection coefficient.

Studies of the complete flow field by the method of characteristics show that, once the reflected waves from an incident shock wave reach the surface, the asymptotic surface pressure p_∞ is approached rapidly. This gives some support to the use, for two-dimensional sharp edged bodies in hypersonic flow, of the methods that relate the surface pressure to the freestream conditions and the local surface slope. These methods effectively assume that the asymptotic pressure p_∞

Table 2 Pressure drag coefficient of cylinder-flare combination

Nose shape	C_D
Conical 5° semi-angle	0.455
Conical 10° semi-angle	0.441
Conical 20° semi-angle	0.366
Conical 30° semi-angle	0.361
Conical 45° semi-angle	0.382
Hemispherical	0.352

is reached instantaneously, whereas the shock-expansion approach assumes that the pressure p_i immediately downstream of the discontinuity is unaffected by reflected waves.

The concept of a reflection coefficient also can be applied to the reflected waves that are produced when the wave from a surface discontinuity interacts with the entropy gradient behind the curved shock wave over a blunt nose. Well downstream of the nose on a body with parallel sides at zero incidence, this entropy gradient takes the form of a positive Mach number gradient normal to the surface in an almost constant pressure flow. At low supersonic speeds, this gradient is such that the freestream Mach number is reached effectively several nose radii away from the surface. However, at hypersonic speeds, not only is the surface Mach number a much smaller fraction of the freestream Mach number, but the gradient normal to the surface is extremely small. Therefore, although the reflection coefficient can be very large at hypersonic speeds, the rate of approach to the asymptotic pressure is, in most practical cases, so slow that the reflected waves will have little effect on the pressure distribution downstream of a discontinuity. This means that, contrary to the conclusions for the sharp-nosed bodies, any attempt to estimate the surface pressure on a complex blunt-nosed hypersonic body from the local surface slope and the freestream conditions is likely to lead to most inaccurate results.

One result of this slow approach to the freestream Mach number normal to the surface of a blunt-nosed hypersonic body is that the drag of a flare far downstream on a cylinder with a blunt nose is less than that of a similar one on a cylinder with a sharp nose. To illustrate this effect, calculations have been made of the drag coefficient of a long cylinder followed by a 30° semi-angle conical flare with a base diameter double that of the cylinder. The cylinder-flare combination is in a flow of $M_f = 8$ and $\gamma = \frac{7}{5}$, and a number of nose shapes have been considered. The drag of the nose is included, but base drag is comparatively small and has been neglected. The results are presented in Table 2 and are quite striking in that the drag coefficient of the combination with a conical nose decreases as the nose angle is increased until a minimum is reached at a semi-angle of about 30°, and the drag coefficient of the combination with a hemispherical nose actually is less than the minimum for the conical noses.

In axisymmetric flow, a pressure gradient exists downstream of a discontinuity in surface slope due to the effective change in flow area with distance from the axis. In the case of a cylinder-flare combination with constant flow properties in front of the flare, the asymptotic (i.e., conical) pressure on the flare is reached effectively at a radial distance of about two or three times the radius of the cylinder.

As an example of the application of these two-dimensional and axisymmetric results to three-dimensional flows, consider the experimental results reported by Fitzgerald[8] for the pressure on a cylinder with a 10° conical flare at an incidence of 27° in a stream of $M_f = 8.5$. The two-dimensional results for ϵ at $M_f = 8$ (Fig. 4) show that, for $\delta_1 = 27°$ and $\delta_2 = 10°$, the reflected wave should be an expansion with a pressure difference equal to 0.175 that across the incident shock. This means that the pressure change at the surface for the initial reflection of this reflected wave should be about 0.35 times the pressure difference across the incident shock. The experimental results along the lowest meridian of the three-dimensional body show a pressure drop of just this magnitude when the reflected wave from the intersection of the bow and flare shocks strikes the surface.

References

[1] Hayes, W. D. and Probstein, R. F., *Hypersonic Flow Theory* (Academic Press, New York, 1959).

[2] Waldman. G. D. and Probstein, R. F., "An analytic extension of the shock-expansion method," J. Aerospace Sci. **28,** 119–132 (1961).

[3] Lighthill, M. J., "The flow behind a stationary shock," Phil. Mag. **40,** 214 (1949).

[4] Chu, B. T., "On weak interaction of strong shock and Mach waves generated downstream of the shock," J. Aeronaut. Sci. **19,** 433 (1952).

[5] Courant, R. and Friedrichs, K. O., *Supersonic Flow and Shock Waves* (Interscience Publishers, New York, 1948), pp. 347–350.

[6] Fuller, F. B., "Numerical solutions for supersonic flow of an ideal gas around blunt two-dimensional bodies," NASA TN D-791 (July 1961).

[7] Van Hise, V., "Analytic study of induced pressure on long bodies of revolution with varying nose bluntness at hypersonic speeds," NASA TR R-78 (1960).

[8] Fitzgerald, P. E., "On the influence of secondary waves from the intersection of shocks of the same family," J. Aerospace Sci. **29,** 755 (1962).